Brief Communication

Functional maturation and longitudinal imaging of intraportal neonatal porcine islet grafts in genetically diabetic pigs

Johanna Pilz [1,2,3,†], Nicol Gloddek [1,2,3,†], Felix Lindheimer [4],
Magdalena J. Lindner [4], Daniel Puhr-Westerheide [5], Muzzafer Ümütlü [5],
Clemens Cyran [5], Max Seidensticker [5], Richard Lindner [1,2,3],
Martin Kraetzl [1,2,3], Simone Renner [1,2,3], Daphne Merkus [6], Daniel Teupser [7],
Peter Bartenstein [4], Sibylle I. Ziegler [4], Eckhard Wolf [1,2,3],
Elisabeth Kemter [1,2,3,*]

[1] Chair for Molecular Animal Breeding and Biotechnology, Gene Center and Department of Veterinary Sciences, LMU Munich, Munich, Germany
[2] Center for Innovative Medical Models, Department of Veterinary Sciences, LMU Munich, Munich, Germany
[3] German Center for Diabetes Research (DZD), Neuherberg, Germany
[4] Department of Nuclear Medicine, University Hospital, LMU Munich, Munich, Germany
[5] Department of Radiology, University Hospital, LMU Munich, Munich, Germany
[6] Walter Brendel Center for Experimental Medicine (WBex), University Hospital, LMU Munich, Munich, Germany
[7] Department of Laboratory Medicine, University Hospital, LMU Munich, Munich, Germany

A B S T R A C T

Allogeneic intraportal islet transplantation (ITx) has become an established treatment for patients with poorly controlled type 1 diabetes. However, the loss of viable beta-cell mass after transplantation remains a major challenge. Therefore, noninvasive imaging methods for long-term monitoring of the transplant fate are required. In this study, [68Ga]Ga-DOTA-exendin-4 positron emission tomography/computed tomography (PET/CT) was used for repeated monitoring of allogeneic neonatal porcine islets (NPI) after intraportal transplantation into immunosuppressed genetically diabetic pigs. NPI transplantation (3320-15,000 islet equivalents per kg body weight) led to a reduced need for exogenous insulin therapy and finally normalization of blood glucose levels in 3 out of 4 animals after 5 to 10

weeks. Longitudinal PET/CT measurements revealed a significant increase in standard uptake values in graft-bearing livers. Histologic analysis confirmed the presence of well-engrafted, mature islet clusters in the transplanted livers. Our study presents a novel large animal model for allogeneic intraportal ITx. A relatively small dose of NPIs was sufficient to normalize blood glucose levels in a clinically relevant diabetic pig model. [^{68}Ga]Ga-DOTA-exendin-4 PET/CT proved to be efficacious for longitudinal monitoring of islet transplants. Thus, it could play a crucial role in optimizing ITx as a curative therapy for type 1 diabetes.

1. Introduction

Allogeneic percutaneous intraportal pancreatic islet transplantation (ITx) is a validated therapy for patients with type 1 diabetes (T1D) suffering from uncontrolled episodes of hyper- and hypoglycemic events, also called brittle diabetes.[1-3] However, there is a decline in islet graft function over time and the underlying mechanisms are often unclear.[4] Clinical assessment of islet grafts is so far limited to measuring metabolic parameters such as blood glucose variability, frequency of hypoglycemic events, C-peptide or HbA$_{1c}$ levels, or a combination, eg, in the BETA2 score.[5] Noninvasive imaging of viable beta cells in the islet graft would help to clarify if a patient needs additional islet loading or if graft rejection is ongoing. Up-to-date, few 1-time islet imaging studies were done either in the early posttransplant period to monitor immediate graft loss, or in graft-bearing patients after reaching a normoglycemic state.[6-11] However, to obtain insights into changes in graft mass over time, longitudinal measurements are necessary.

Novel beta-cell replacement therapies are mainly tested in rodents with toxin-induced diabetes[12] or in nonhuman primates (NHPs),[13,14] both associated with limitations in translating findings to human patients. Therefore, this study used *INS*^{C94Y} transgenic pigs, a model for mutant *INS* gene-induced diabetes of youth (MIDY), showing early onset of diabetes and requiring daily insulin (INS) treatment,[15] similar to patients with MIDY.[16] Neonatal porcine islets (NPIs) are an attractive xenogeneic source for beta-cell replacement therapy.[17] In a recent small animal positron emission tomography/computed tomography (PET/CT) study, specific binding of radiolabelled exendin-4 on porcine NPI grafts was demonstrated.[18] Therefore, [^{68}Ga]Ga-,4,7,10-tetraazacyclo-dodecane-1,4,7,10-tetraacetic acid (DOTA)-exendin-4 PET/CT was performed in MIDY pigs to longitudinally monitor the fate of intraportal NPI grafts and correlate the imaging data with improvements in glucose control and quantitative histologic analyses of islet grafts in recipient livers.

2. Methods

2.1. Establishment of a porcine islet allotransplantation model in diabetic pigs

NPIs were isolated from pancreata of 1- to 7-day-old wild-type piglets and in vitro matured for 6 to 7 days.[19] Table 1 contains the NPI culture and transplantation media used. Minimally invasive percutaneous intraportal pancreatic ITx (PIPIT)[20] was performed in anesthetized 12- to 18-week-old MIDY pigs (n = 4). The immunosuppressive regimen was based on tacrolimus and mycophenolate mofetil accompanied by an antithrombotic therapy (Table 2). NPIs were resuspended in the transplantation medium shortly before intraportal infusion. After ultrasound-guided transhepatic access to the portal vein, a catheter was placed in the left portal vein branch in 3 animals, and in the main branch of the portal vein in the fourth animal. Correct catheter position was controlled by angiography. After NPI administration, the access tract was embolized using gelfoam sludge. Serum aspartate aminotransferase post-PIPIT and fasting blood glucose (FBG) values were measured as described.[21] INS therapy using long-acting (Lantus, Sanofi) and short-acting (NovoRapid, Novo Nordisk) INS analogs (long-acting insulin analog [LAIA] and short-acting insulin analog [SAIA]) was adjusted to reach FBG levels of ≤200 mg/dL. Values of >200 mg/dL determined the starting point of INS therapy.

All animal experiments were performed according to the German Animal Welfare Act and were approved by the responsible animal welfare authority (Government of Upper Bavaria). Pigs had free access to tap water and were fed once per day (Breeding-feed-LMU, Vilstalmühle) together with INS application.

2.2. Longitudinal [^{68}Ga]Ga-DOTA-exendin-4 PET/CT imaging of NPI grafts

Animals were imaged with [^{68}Ga]Ga-DOTA-exendin-4 (18) once before ITx (baseline) and up to 3 times in the posttransplant period. PET/CT was performed under anesthesia (Table 2). Technical settings for [^{68}Ga]Ga-DOTA-exendin-4 PET/CT imaging are shown in Table 3.

2.3. PET/CT image analysis

Reconstructed PET/CT data were analyzed using PMOD software (version 4.005, PMOD Technologies). In each data set, whole-organ liver volumes were manually segmented in the PET images. In addition, small spherical regions were used to determine activity concentrations in the pancreas, kidney, liver, and longissimus dorsi muscle for reference. Mean values of the activity concentrations in these volumes were extracted for each time point in the dynamic PET acquisition. For standardized

Table 1

NPI culture and transplantation media.

Recovery media (day 0 and day 1 of culture)	
1:1 mixture of Ham's F12 and medium 199	#M4530 and #M4530, Sigma
0.5% BSA	#A9418, Sigma
10 mmol/L glucose	#G7021, Sigma
10 mmol/L L-glutamine	#G8540, Sigma
10 mmol/L HEPES	#15630-056, Gibco
10 mmol/L nicotinamide	#N0636, Sigma
0.062% glutathione	#G6013, Sigma
1x penicillin/streptomycin	#15140-122, Gibco
1x amphotericin	#15290-026, Gibco
25 U/mL heparin	#H3149, Sigma
0.5 mmol/L Pefabloc	#0031682.02, Serva
100 KIU aprotinin	#A3428, Sigma
10 µmol/L Trolox	#238813, Sigma
1x BME vitamins	#B6891, Sigma
15.2 µmol/L zinc sulfate	#Z0251, Sigma
1 µmol/L liraglutide	Victoza 6 mg/mL, Novo Nordisk
1x ITS supplement	#41400-045, Invitrogen
Maturation media (day 3 onwards)	
Ham's F10	#N6908, Sigma
0.5% BSA	#A9418, Sigma
10 mmol/L glucose	#G7021, Sigma
10 mmol/L L-glutamine	#G8540, Sigma
10 µmol/L IBMX	#I5879, Sigma
10 mmol/L nicotinamide	#N0636, Sigma
1x penicillin/streptomycin	#15140-122, Gibco
1.6 mmol/L CaCl$_2$	#C7902, Sigma
1 µmol/L liraglutide	Victoza 6 mg/mL, Novo Nordisk
1 µmol/L T3 analog	#5552, Tocris
50 nmol/L retinoic acid	#0695, Tocris
Transplantation media	
CMRL-1066	#P04-84600, PAN Biotech
0.5% human albumin	Alburex20%, CSL Behring
70 U/kg body weight heparin	Heparin-Natrium 5.000 I.E./mL, Braun

uptake values (SUVs), activity concentration values were normalized to injected radioactivity and body weight (BW).

For each transplant recipient, the course of whole liver SUVs was analyzed from baseline measurements to posttransplant measurements up to day 98. Whole liver SUVs were analyzed 55 minutes after tracer injection.

In addition, a hotspot analysis of the liver volume was performed.[11] The mean and SD value of the baseline SUVs at 55 minutes after injection in the liver were calculated and a "hotspot" threshold was defined as mean + 2 (SD). With this cutoff value (0.47), hotspot regions were identified using PMOD isocontouring. The development of average values of activity concentration in the hotspot regions was determined for all collected measurements from baseline up to 98 days.

2.4. Sampling procedure and histologic analysis

Within 1 week after the last PET/CT, systematic sampling of the liver was done (Supplementary Figure). Formalin-fixed, paraffin-embedded sections were immunohistochemically stained for synaptophysin (SYP), INS, and glucagon (GCG) as detailed in Supplementary Table S1. SYP-positive cell clusters excluding neuronal cells and nerves were scored in 4 grades (none vs 1-5 vs 6-15 vs >15 islet cell clusters [ICCs] per section). Representative sections were also investigated by 4-color immunofluorescence staining of SYP-, INS-, GCG-, and so-matostatin (SST)-positive cells (for technical details, see Supplementary Table S2). Image acquisition was performed using Axioscan 7 and 20× objective.

2.5. Statistical analysis

SUV data were analyzed using PROC MIXED (SAS 9.4; SAS Institute), taking the effect of time after transplantation and the random effect of the individual recipient into account.

3. Results

3.1. Intraportally transplanted NPI allografts cure diabetes of MIDY pigs

Four MIDY pigs received 3320- to 15,000 islet equivalents (IEQs) NPIs per kg BW by PIPIT at an age between 81 and 137 days and a BW between 20 to 50 kg (Fig. 1). FBG concentrations were 200 mg/dL in 1 animal and around 300 mg/dL in the other 3. Three pigs received daily INS treatment before PIPIT, whereas in the fourth animal, INS treatment started at PIPIT.

After PIPIT, pig #13062 reached normoglycemia (FBG < 110 mg/dL) for the first time at day 18 and consistent normoglycemia on day 64. SAIA was omitted on day 32 and LAIA on day 54. Pig #12580 had a similar course (first and consistent normoglycemia at day 47 and day 72, respectively; 1 elevated value (132 mg/dL) on day 94; omission of SAIA at day 45 and of LAIA at day 100). Pig #12582 showed normoglycemia for the first time at day 23 and stayed in a near normoglycemic range (110-141 mg/dL) from day 37 onward. SAIA was discontinued on day 16, but 2 IU of LAIA was constantly administered from day 61. Pig #13064 mostly exhibited FBG levels of <200 mg/dL as of week 4. INS treatment plateaued from day 29 at 10 to 11 IU LAIA/3 IU SAIA per day (Fig. 2).

Table 2

Medical treatment of graft-recipient pigs.

Indication	Agent	Dose	Application route	Brand
Anesthesia at PIPIT				
Induction	Azaperone	10 mg/kg BW	i.m.	Stresnil; Elanco Animal Health
	Ketamine	20 mg/kg BW	i.m.	Ketamidor; WDT
Maintenance	Sevoflurane	1%-2%	inhalation	SEVOrane; AbbVie
Analgesia at peri-PIPIT time period				
Preemptive at PIPIT	Morphasol	0.01 mL/kg BW	i.v.	Morphasol, 4 mg/mL; Livisto
	Meloxicam	0.4 mg/kg BW	i.m.	Metacam 20 mg/mL, Boehringer Ingelheim
Postoperative	Meloxicam	0.4 mg/kg BW	i.m., at day 1 post-PIPIT	Metacam 20 mg/mL, Boehringer Ingelheim
Immunosuppressive and antithrombotic therapy				
Immunosuppression	Tacrolimus	0.25 mg/kg BW	oral twice daily, from day 1 till end	Prograf 5 mg; Astellas Pharma GmbH
	Mycophenolate mofetil	500 mg	oral twice daily, from day 1 till end	CellCept 1 g/5 mL; Roche
Anticoagulation	Acetylsalicylic acid	100 mg	oral, from day 1 till end	Aspirin; Bayer
	Heparin	36 U/kg BW	i.v. once at PIPIT	Heparin-Natrium 5000 IU/mL; Braun
			s.c. 3 injections every 12 h after PIPIT	
Anesthesia at [68Ga]Ga-DOTA-exendin-4 PET/CT imaging				
Induction	Azaperone	10 mg/kg BW	i.m.	Stresnil; Elanco Animal Health
	Ketamine	20 mg/kg BW	i.m.	Ketamidor; WDT
Maintenance	Xylazine	1 mg/kg BW	i.v.	Rompun 2%; Bayer Vital GmbH
	Ketamine	20 mg/kg BW	i.v.	Ketamidor; WDT

Blood glucose concentration, heart function, and blood oxygen saturation were continuously monitored during anesthesia.

BW, body weight; DOTA, 1,4,7,10-tetraazacyclododecane-1,4,7,10-tetraacetic acid; i.m., intramuscular; i.v., intravenous; PET/CT, positron emission tomography/computed tomography; PIPIT, percutaneous intraportal pancreatic islet transplantation; s.c., subcutaneous.

3.2. Time-activity curve analysis of [68Ga]Ga-DOTA-exendin-4 PET/CT scan revealed accumulation of radiotracer in pig pancreas

No adverse effects in pigs were observed after intravenous application of [68Ga]Ga-DOTA-exendin-4. Time-activity curves of the mean SUV showed rapid uptake of the tracer in the pancreas, kidneys, and liver, whereas the uptake in the muscle stayed constantly at the background level (Fig. 3A, B). Within a few minutes after application, the highest tracer accumulation was present in the kidneys (excretory organs). Distinct signal accumulation was detected in the pancreas, reaching a plateau SUV level between 2.5 and 5.2 after 36 minutes. Liver SUVs ranged initially between 2.5 and 3.9 and decreased to values below 1 after 30 minutes.

3.3. Increase of SUV in NPI graft–bearing livers in longitudinal [68Ga]Ga-DOTA-exendin-4 PET/CT occurs together with graft function in MIDY pigs

Average baseline SUV of livers was 0.46 (range, 0.39-0.52) (Fig. 3C), reflecting the background uptake of [68Ga]Ga-DOTA-exendin-4. After PIPIT, whole liver SUV continuously and significantly increased during the observation period. In particular,

animals #13062 and #12580 showed a steady increase of liver SUV by 66% and 115% at their last vs their first scans, whereas for pig #12582, an initial rise in SUV (by 111%) was recorded, which then plateaued. In #13064, only a minor increase (12%) in liver SUV was noted (Fig. 3C). The hotspot analysis revealed a continuous increase in measured SUV after ITx in all PET/CT scans of pigs #13062, #12580, and #12582 (42%, 50% and 127%, respectively). In contrast, there was almost no SUV increase in animal #13064 (2%) (Fig. 3D). An example of coronal slices of [68Ga]Ga-DOTA-exendin-4 PET/CT of animal #13062 once before PIPIT, on day 54 and day 89 post-PIPIT showed an intensified liver signal, which was multifocal with distinct regions of strong hepatic uptake (Fig. 3E).

3.4. Histologic evaluation of NPI graft–bearing livers revealed a multifocal distribution of well-engrafted and matured islet clusters

NPI grafts, identified in liver slides by SYP immunostaining, were enriched in the left liver lobes of animals #12580, #12582, and #13064, whereas animal #13062 showed a more diffuse graft distribution among all liver lobes (Fig. 4A). On average, 31% of the sections contained 1 to 5 SYP-positive ICCs, 8% between 6 to 15 ICCs, and 1% had ≥15 ICCs. The cross-sectional area of

Table 3

Technical settings for [^{68}Ga]Ga-DOTA-exendin-4 PET/CT imaging in pigs.

Tracer application	
Route:	i.v. via an ear vein catheter
Dose of [^{68}Ga]Ga-DOTA-exendin-4:	24.66-91.37 MBq; 0.02 $\pm$ 0.005 µg peptide/kg BW
Time interval between synthesis and injection:	34 min on average
Technical settings for PET/CT image acquisition	
Apparatus:	Biograph True-Point 64 PET/CT device (Siemens)
Mode of action:	dynamic PET/CT scan
Axial field-of-view:	21.6 cm, with focus on the region of the liver
Start of PET acquisition:	1 min before tracer injection
List-mode data acquisition:	over 60 min, sorted into 24 frames (11 $\times$ 1 min, 10 $\times$ 2 min, 3 $\times$ 10 min)
Technical settings for PET/CT image analysis	
Software:	TrueX, Siemens
Algorithm settings:	3 iterations and 21 subsets (voxel size [x, y, z]: 2.67, 2.67, 3.0 [mm^3])
	including corrections for scattered radiation and attenuation
Filter settings:	Gaussian filter with 5 mm full width at half maximum

For anatomical information and scatter as well as attenuation correction, low-dose CT scans without contrast agents were acquired for the liver and the whole-body regions.
BW, body weight; DOTA, 1,4,7,10-tetraazacyclododecane-1,4,7,10-tetraacetic acid; PET/CT, positron emission tomography/computed tomography.

the clusters ranged from 0.8 to 113 $\times$ 10^3 µm, with a heterogeneous size distribution over the transplanted liver lobe. NPI clusters were well-engrafted in the periportal area and were fully matured, containing INS-positive beta cells, GCG-positive alpha cells, and SST-positive delta cells (Fig. 4B). NPI graft distribution and incidence of SYP-, INS-, and GCG-containing cells of each NPI recipient pig is shown in Figure 4C. Of the animals that underwent a successful unilateral ITx, an average of 33% of the examined sections contained ICCs, of which 64% were INS-positive and 72% were GCG-positive. In animal #13062, islets were distributed throughout the liver, and ICCs were found in 64% of the examined sections, of which 84% were INS-positive and 81% GCG-positive.
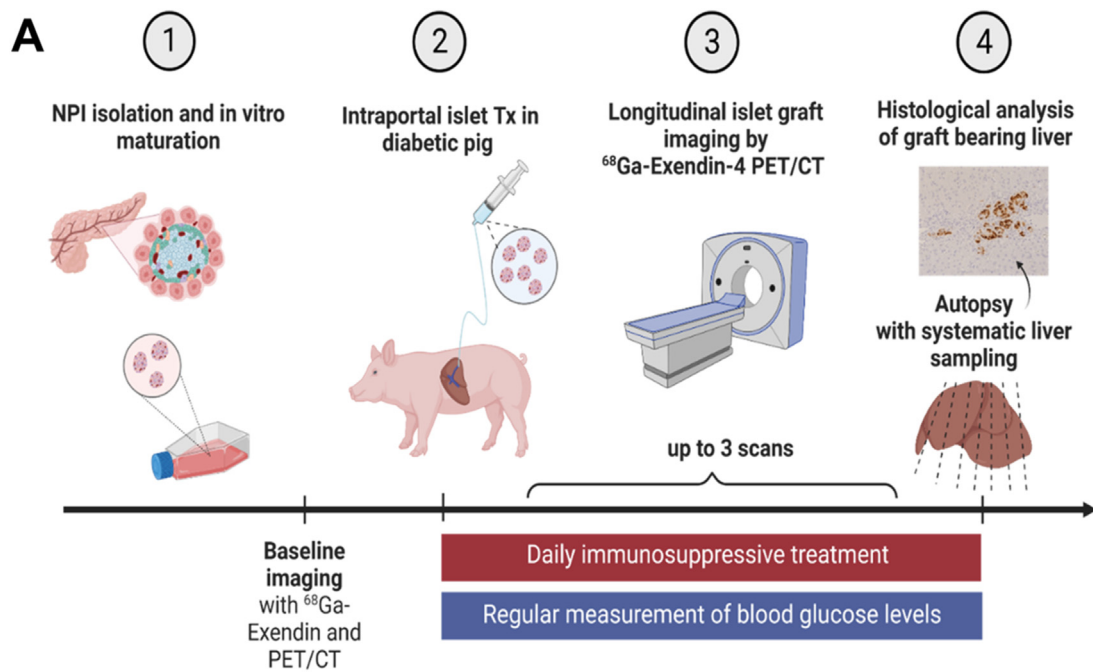
4. Discussion

Preclinical research in the field of ITx is mostly done in rodents. However, body size is of major importance for developing clinically applicable imaging modalities with improved sensitivity and resolution; hence, the translational value of rodent models is limited. Moreover, their pancreatic islet physiology differs from humans.[22] Consequently, NHP models have been used; however, their demand of insulin for glucose control is much higher than in humans.[23] In intrahepatic ITx of pancreatectomized or streptozotocin-induced diabetic NHPs, 100,000 IEQs/kg BW of adult pig islets or 9600 to 56,900 IEQs/kg BW of NPIs were required to achieve normoglycemia.[13,24] The lag time to normalize recipients' blood glucose levels and to come off INS ranged between 20 and 189 days.[13]

In the present study, we used a genetically modified MIDY pig model which gets consistently diabetic without further interventions. PIPIT of 3300 to 9700 IEQs NPIs/kg BW was sufficient to cure diabetes in this model. As immature NPIs were transplanted, in vivo maturation and volume expansion were essential to achieve a critical functional islet graft mass normalizing the recipients' blood glucose levels. In vivo matured NPI grafts in the liver consisted of alpha-, beta-, and delta-cells, resembling the islets of Langerhans in the pancreas and required for proper glucose control. Similar to the findings in NHP ITx models, no correlation between NPI transplant mass and reversal of diabetes was observed. One possible explanation is an instant blood-mediated inflammatory reaction, which may lead to a loss of up to >50% ICCs in the early posttransplant period. Hypoxia-based engraftment failure is another important cause of early islet graft loss.[25] Longitudinal noninvasive islet graft imaging is thus an important asset in ITx, shedding light on the graft fate. Only a few studies performed islet graft imaging in large animal models or clinical settings.

Malosio et al[6] performed magnetic resonance imaging (MRI) in patients after intrahepatic ITx with superparamagnetic iron oxide (SPIO)-labeled islets. From 1 month post-ITx onward, despite functional islet grafts, there was a steady decline in the number of hypointense spots, as seen in other SPIO-MRI ITx studies.[7,8] Importantly, SPIO-MRI does not differentiate viable from dying islets.[9] As SPIO labeling has to be performed before Tx, MRI islet graft imaging is not suitable for long-term islet survival monitoring.

Tracing of islets can also be achieved by [^{18}F]-fluorodeoxyglucose labeling of the islets shortly before ITx and dynamic PET/CT after ITx.[26] Based on this principle, islet distribution in the liver was seen to be heterogeneous, with a marked concentration in small multifocal areas throughout the organ.[10,26] Only 53% of

Figure 1. Overview of study design and characteristics of islet graft-recipient pigs. (A) After neonatal porcine islet (NPI) isolation and in vitro maturation, diabetic recipient pigs (n = 4) received the NPI graft through portal vein infusion. Baseline positron emission tomography/computed tomography (PET/CT) imaging with [^{68}Ga]Ga-DOTA-exendin-4 was performed before transplantation. The post–islet transplantation (ITx) monitoring period was accompanied by daily immunosuppressive treatment and regular measurement of blood glucose levels. Longitudinal PET/CT imaging with [^{68}Ga]Ga-DOTA-exendin-4 was performed once before transplantation and up to 3 times in the post-ITx period. Last tracer imaging was performed a few days before the necropsy, accompanied by systematic liver sampling. Subsequently, the graft-bearing livers underwent detailed histologic analysis. (B) Characteristics of the 4 diabetic islet graft-recipient pigs. NPI donor characteristics: number of piglets used (age in days). AST, aspartate aminotransferase; BW, body weight; IEQ, islet equivalent; IN, insulin treatment; ldIN, low-dose insulin treatment; MIDY, hereditary diabetic pig harboring the mutant *INS*^{C94Y} transgene (created with BioRender.com).

the administered radioactivity was detected in the liver, suggesting half of the transplanted islet cell mass was lost within minutes.[10] Although prelabelling allows us to image the location of transplanted islets, it does not yield information on their viability and long-term changes. In a clinical study, [^{11}C] 5-hydroxytryptophan ([^{11}C]5-HTP, a marker for alpha and beta

cells) was used to image patients after intraportal ITx twice at intervals of 8 months using PET and MRI. Tracer accumulation was detected in hepatic hotspot regions, associated with islet graft function.[27]

The glucagon-like peptide-1 (GLP1) analog exendin-4 binds selectively to GLP1 receptors, which are highly enriched on beta
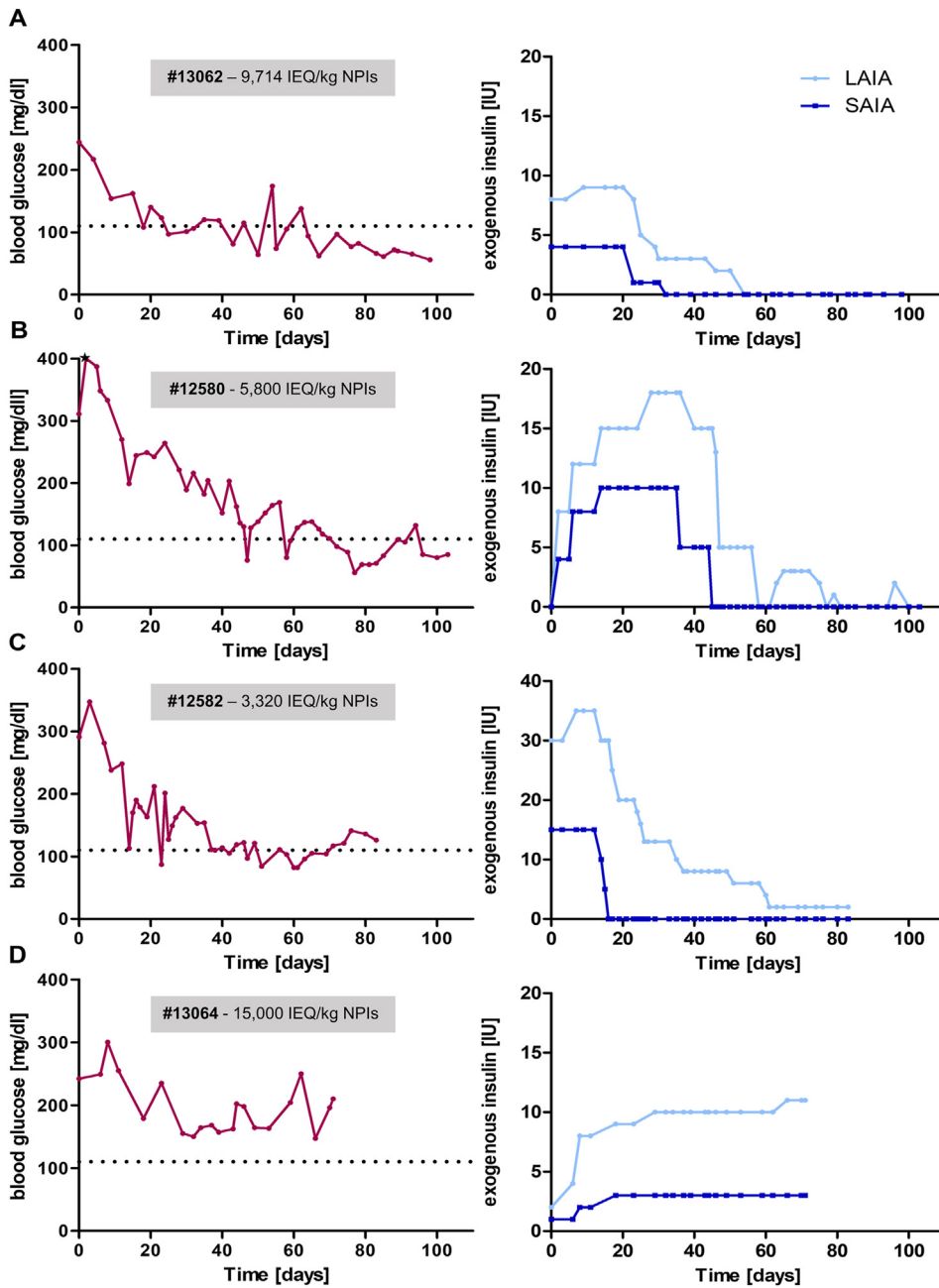
Figure 2. Glycemic profile and exogenous insulin therapy regime during the post–islet transplantation (ITx) monitoring period of the neonatal porcine islet (NPI) graft-recipient MIDY pigs. (A) Pig #13062, 9,714 transplanted islet equivalents (IEQs)/kg body weight (BW), (B) Pig #12580, 5800 transplanted IEQs/kg BW. Animals #12580 and #13062 achieved constant normoglycemia (fasting blood glucose levels consistently <110 mg/dL on days 64 and 72. Independence from insulin treatment occurred on days 54 and 100 after NPI transplantation. (C) Pig #12582, 3320 transplanted IEQs/kg BW. NPI graft–recipient pig #12582 had a constant reduction of blood glucose levels to a normoglycemic level and a reduction of exogenous insulin dose. (D) Pig #13064, 15,000 transplanted IEQs/kg BW. Animal #13064 exhibited a reduction of blood glucose levels constantly <200 mg/dL as of week 4 after NPI transplantation. Exogenous insulin dose plateaued from day 29 post-ITx.

cells. By the accumulation of radioactively labeled exendin-4 upon receptor binding and complex internalization, in vivo labeling and specific imaging of viable human, murine, and porcine beta cells by PET/CT is possible.[18] Studies in rodents using single photon emission computed tomography demonstrated a linear correlation of exendin tracer signal with beta-cell mass.[28] In a recent proof-of-concept study, 9 patients with functional islet grafts at least 6 months after ITx underwent a [68Ga]Ga-NODAGA-exendin-4-PET/CT scan.[11] As controls, scans of 4 patients with T1D without islet grafts were used; among them, 1 patient received an islet graft later and was thus also in the ITx group. Graft-bearing livers displayed distinct regions with strong hepatic uptake, defined as hotspots. The total distribution volume of [68Ga]Ga-NODAGA-exendin-4 in hotspot regions was significantly higher in the ITx group compared to the control group (median

0.55 vs 0.43). No correlation was found between the [68Ga]Ga-NODAGA-exendin-4 PET-derived signal and the IEQs ITx mass or metabolic parameters in the islet graft recipients. The liver SUV in the control group (1.3 ± 0.2) was strikingly higher compared to the baseline SUV of the pigs in our study. Because exendin is a relatively large peptide, both compounds only differ in the chelators used, which are very similar (NODAGA and DOTA). The differences in binding affinity caused by the chelators are unlikely to be significant; hence, the contrast between the SUVs is most likely caused by species differences between humans and pigs.

In contrast to this proof-of-concept study with only 1 assessment, we performed a longitudinal study with a baseline and up to 3 follow-up [68Ga]Ga-DOTA-exendin-4 PET/CT investigations in a newly established diabetic ITx large animal model. GLP1
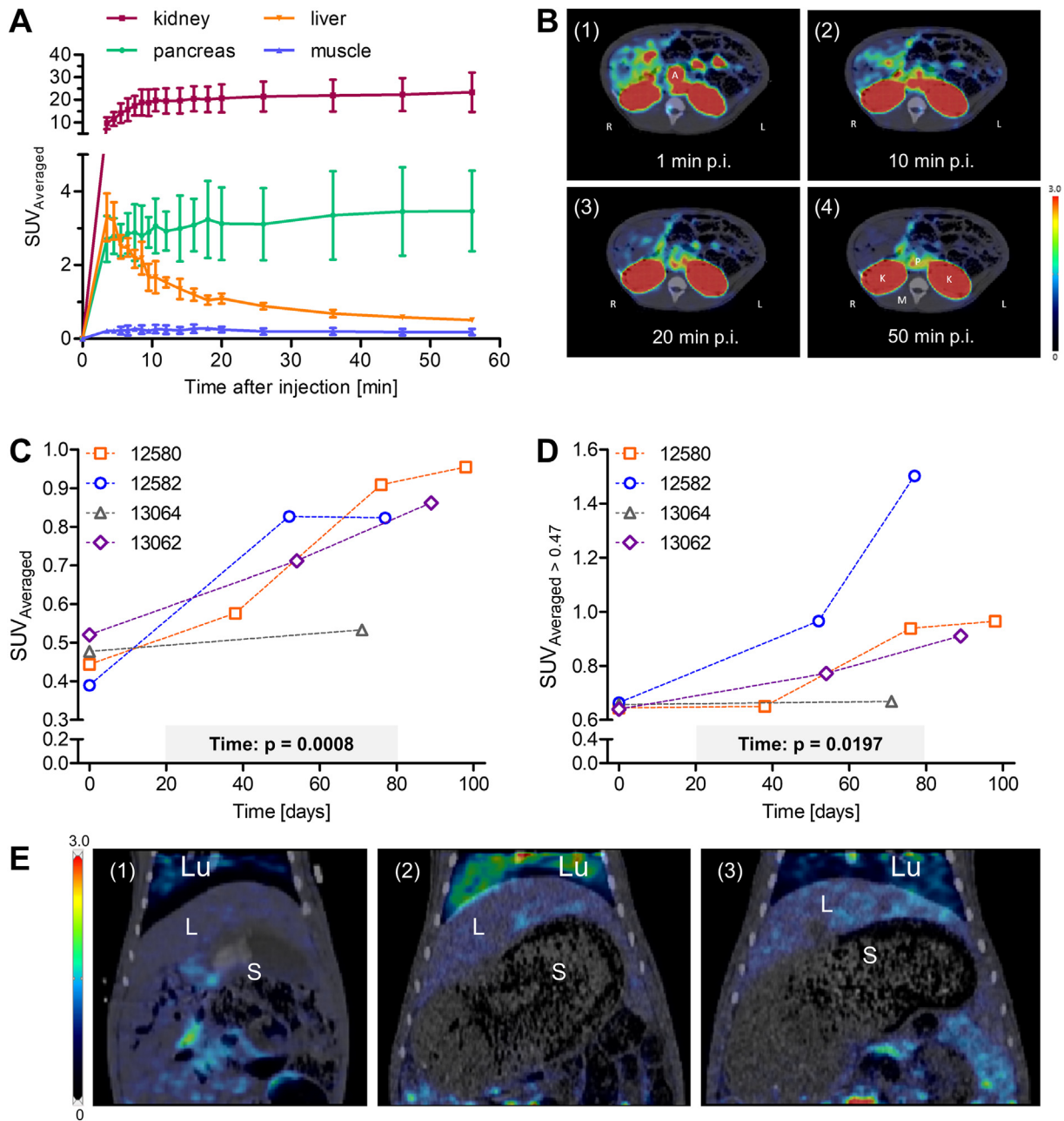
Figure 3. [^{68}Ga]Ga-DOTA-exendin-4-PET/CT. (A) Proof of concept: time-activity curves of [^{68}Ga]Ga-DOTA-exendin-4 within 60 minutes after injection. Shown is the mean standardized uptake value (SUV) of the pigs #12580, #12582, #13062, and #13064 measured in the baseline scans. Mean SUV was measured in kidneys, liver, pancreas, and longissimus dorsi muscle. (B) Examples of axial [^{68}Ga]Ga-DOTA-exendin-4 PET/CT images at 1 minute (1; A: aorta), 10 minutes (2), 20 minutes, and (3) 55 minutes (4) after injection (pig #13062), normalized to (SUV) = 3. [^{68}Ga]Ga-DOTA-exendin-4 can be detected in the kidneys (K) (excretory organs) and in the pancreas (P) (positive control). No accumulation in the longissimus dorsi (M) (negative control). (C) Development of whole liver SUV$_{Averaged}$ at 55 minutes after injection of [^{68}Ga]Ga-DOTA-exendin-4 from baseline to imaging timepoints up to 98 days post–islet transplantation (ITx) in each graft-recipient pig. Increase of whole liver SUV$_{Averaged}$ in animals #12580, #12582, and #13062. Whole liver SUV$_{Averaged}$ of animal #13064 shows a plateau. (D) Development of SUV$_{Averaged > 0.47}$ in hotspot regions (threshold: 0.47) from baseline scans to imaging time points up to 98 days post-ITx. Hotspot SUV$_{Averaged > 0.47}$ increases in animals #12580, #12582, and #13062. Hotspot SUV$_{Averaged > 0.47}$ of animal #13064 shows a plateau. (E) Comparison of PET/CT at the last frames 55 minutes after administration of ^{68}Ga-exendin-4 in pig #13062 before transplantation (1) and on ITx day 54 (2) and ITx day 89 (3) indicates diffuse multifocal increase in liver signal. To enable direct comparison, coronal images are normalized to SUV = 3.

receptor expression is selectively present on the beta cells of the pig pancreas.[29] In our MIDY pig model, beta-cell mass is initially normal, but INS secretion is impaired. Over time, beta-cell mass decreases due to endoplasmic reticulum stress and apoptosis.

At the age of the pigs used in our study, still ~40% of the normal beta-cell mass is present,[15] explaining the high SUV levels in the pancreas. Binding of [^{68}Ga]Ga-DOTA-exendin-4 to NPIs xenotransplanted into the muscle of NOD-SCID IL2r$\gamma^{-/-}$
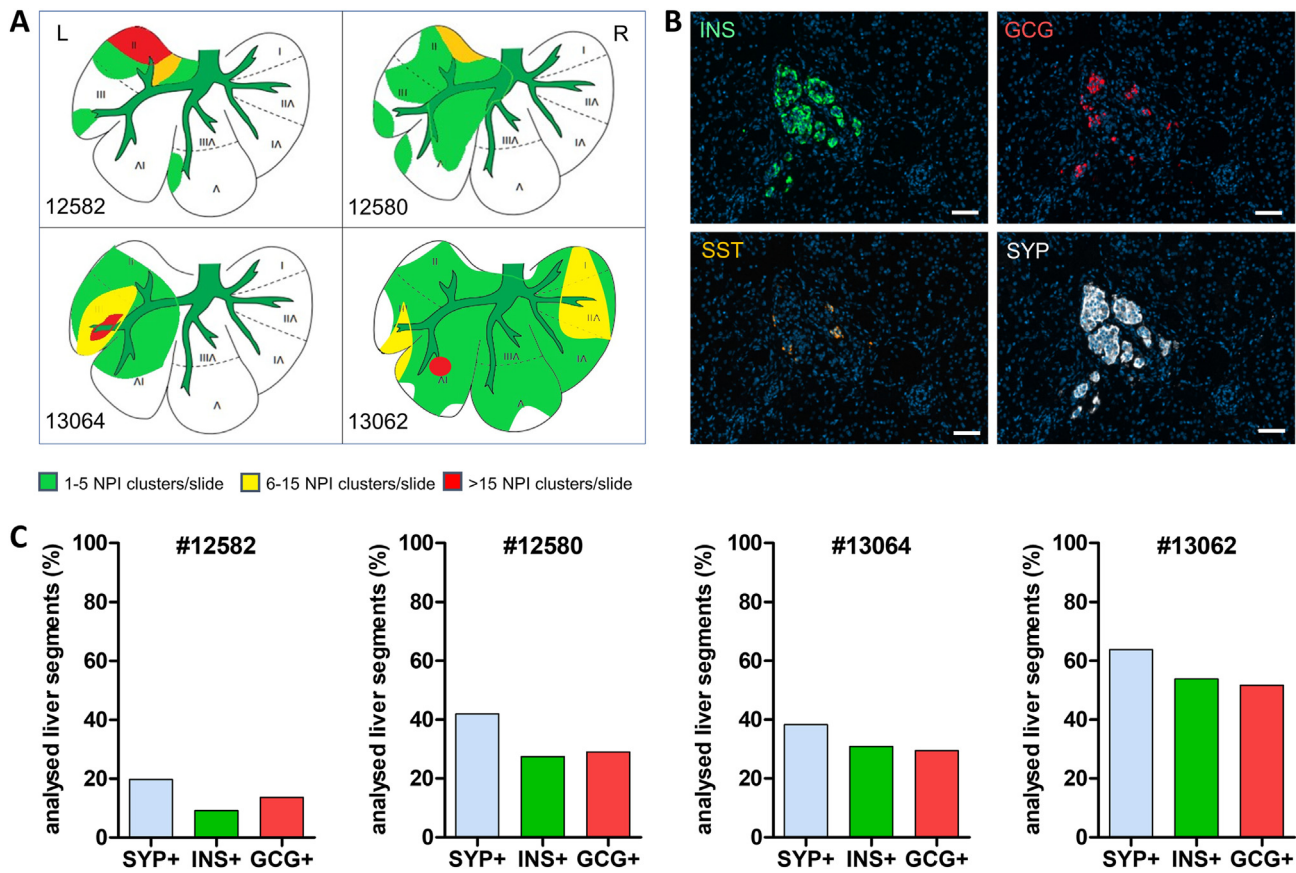
Figure 4. Histologic analysis of graft-bearing livers with immunohistochemistry and immunofluorescence. (A) Distribution and incidence of transplanted islet cell clusters in the whole liver. #12582, #12580, and #13064 show unilateral distribution of the islet graft. In #13062, islet cell clusters were distributed over the whole liver. On average, 244 liver samples from each animal were taken, thereof 72 PFA-fixed liver samples. Islet clusters were identified by SYP immunostaining in 3 μm thick slides of PFA-fixed paraffin-embedded liver samples. (B) Characterization and level of maturation of transplanted islets. Immunofluorescence of insulin (INS), glucagon (GCG), somatostatin (SST), and synaptophysin (SYP) in representative engrafted islet from mutant *INS* gene-induced diabetes of youth (MIDY) pig #13064 in the liver 71 days after islet transplantation (ITx). In blue, cell nuclei counterstained by 4',6-dia-midinod-2-phenylindole (DAPI). Bars = 50 μm. (C) Proportion of SYP-, INS-, and GCG-positive liver segments, based on evaluation of immunohistochemistry.

mice[30] was recently demonstrated by PET/CT.[18] In the present study in pigs, a diffuse increase of the SUV of the whole liver and the occurrence of a hotspot pattern characteristic for viable islet grafts was observed, in line with previous findings in SPIO-MRI, [18F]-fluorodeoxyglucose PET/CT and [68Ga]Ga-DOTA-exendin-4 PET/CT studies in intrahepatic ITx. Because the spatial resolution of clinical PET/CT scanners is in the range of 3 to 4 mm, engrafted clusters of at least 10-fold smaller size cannot individually be resolved due to technical limitations. The identification of individual ICCs with PET/CT is further complicated by the very small graft volume sufficient to cure diabetes compared to the total volume of the liver. Nevertheless, longitudinal PET/CT showed significantly increased SUV values in 3 animals, both in the whole liver and in defined hotspot regions. Furthermore, the multifocal signal enhancements on the coronal images correspond to the distribution pattern of the signal that was also detected in previous studies. The increase of SUV after ITx appeared almost simultaneously with the decrease in blood glucose. Of note, in pig #13064, which did not get normoglycemic and had increased aspartate aminotransferase value post-PIPIT, only a faint increase below the 2 SD threshold of background

signal in both whole liver and hotspot SUV was detected. This indicates that although mature ICCs were found, no critical beta-cell mass for graft function was achieved, which may be due to insufficient engraftment. Therefore, these findings emphasize that an assessment of the change in viable beta-cell mass analogous to graft function can be detected with PET/CT using [68Ga]Ga-DOTA-exendin-4.

5. Conclusion

In summary, our study represents a novel large animal ITx model that, due to its high transferability, is an important link between research and clinical practice, both in questions of ITx and in terms of noninvasive long-term monitoring of islet transplants. Thus, it could play a crucial role in optimizing ITx as a curative therapy for T1D.

Acknowledgments

excellent technical assistance. The authors would also like to thank Dr Mehdi Shakarami, and his animal keeper team for the excellent care of our laboratory animals. Additionally, The authors would like to express their gratitude to the Core Facility Pathology & Tissue Analytics at the Helmholtz Center Munich for their contribution to creating whole slide images.

Data availability

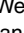All data generated or analyzed during this study are included in this published article.
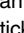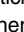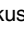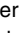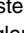
Declaration of competing interest

The authors of this manuscript have no conflicts of interest to disclose as described by the American Journal of Transplantation.

Appendix A. Supplementary data

Supplementary data to this article can be found online at https://doi.org/10.1016/j.ajt.2024.02.026.

ORCiD

Johanna Pilz https://orcid.org/0009-0007-7266-1894
Nicol Gloddek https://orcid.org/0009-0001-2229-8034
Felix Lindheimer https://orcid.org/0009-0002-6904-2623
Daniel Puhr-Westerheide https://orcid.org/0000-0003-3669-5572
Clemens Cyran https://orcid.org/0000-0001-5630-6242
Max Seidensticker https://orcid.org/0000-0002-2481-5410
Richard Lindner https://orcid.org/0000-0003-1836-5377
Martin Kraetzl https://orcid.org/0000-0002-8449-177X
Simone Renner https://orcid.org/0000-0002-5866-4577
Daphne Merkus https://orcid.org/0000-0002-4852-831X
Daniel Teupser https://orcid.org/0000-0001-9843-0145
Peter Bartenstein https://orcid.org/0009-0005-0734-4994
Sibylle I. Ziegler https://orcid.org/0000-0002-5321-4817
Eckhard Wolf https://orcid.org/0000-0002-0430-9510
Elisabeth Kemter https://orcid.org/0000-0001-7785-7502

References

1. Shapiro AM, Lakey JR, Ryan EA, et al. Islet transplantation in seven patients with type 1 diabetes mellitus using a glucocorticoid-free immunosuppressive regimen. *N Engl J Med.* 2000;343(4):230–238. https://doi.org/10.1056/NEJM200007273430401.
2. Marfil-Garza BA, Imes S, Verhoeff K, et al. Pancreatic islet transplantation in type 1 diabetes: 20-year experience from a single-centre cohort in Canada. *Lancet Diabetes Endocrinol.* 2022;10(7):519–532. https://doi.org/10.1016/S2213-8587(22)00114-0.
3. Hering BJ, Ballou CM, Bellin MD, et al. Factors associated with favourable 5 year outcomes in islet transplant alone recipients with type 1 diabetes complicated by severe hypoglycaemia in the Collaborative Islet Transplant Registry. *Diabetologia.* 2023;66(1):163–173. https://doi.org/10.1007/s00125-022-05804-4.
4. Chetboun M, Drumez E, Ballou C, et al. Association between primary graft function and 5-year outcomes of islet allogeneic transplantation in type 1 diabetes: a retrospective, multicentre, observational cohort study in 1210 patients from the Collaborative Islet Transplant Registry. *Lancet Diabetes Endocrinol.* 2023;11(6):391–401. https://doi.org/10.1016/S2213-8587(23)00082-7.
5. Cantley J, Eizirik DL, Latres E, Dayan CM. Islet cells in human type 1 diabetes: from recent advances to novel therapies - a symposium-based roadmap for future research. *J Endocrinol.* 2023;259(1):e230082. https://doi.org/10.1530/JOE-23-0082.
6. Malosio ML, Esposito A, Brigatti C, et al. MR imaging monitoring of iron-labeled pancreatic islets in a small series of patients: islet fate in successful, unsuccessful, and autotransplantation. *Cell Transplant.* 2015;24(11):2285–2296. https://doi.org/10.3727/096368914X684060.
7. Toso C, Vallee JP, Morel P, et al. Clinical magnetic resonance imaging of pancreatic islet grafts after iron nanoparticle labeling. *Am J Transplant.* 2008;8(3):701–706. https://doi.org/10.1111/j.1600-6143.2007.02120.x.
8. Saudek F, Jirák D, Girman P, et al. Magnetic resonance imaging of pancreatic islets transplanted into the liver in humans. *Transplantation.* 2010;90(12):1602–1606. https://doi.org/10.1097/tp.0b013e3181ffba5e.
9. Arifin DR, Bulte JWM. In vivo imaging of pancreatic islet grafts in diabetes treatment. *Front Endocrinol (Lausanne).* 2021;12:640117. https://doi.org/10.3389/fendo.2021.640117.
10. Eich T, Eriksson O, Lundgren T. Nordic Network for Clinical Islet Transplantation. Visualization of early engraftment in clinical islet transplantation by positron-emission tomography. *N Engl J Med.* 2007;356(26):2754–2755. https://doi.org/10.1056/NEJMc070201.
11. Jansen TJP, Buitinga M, Boss M, et al. Monitoring β-cell survival after intrahepatic islet transplantation using dynamic exendin PET imaging: a proof-of-concept study in individuals with type 1 diabetes. *Diabetes.* 2023;72(7):898–907. https://doi.org/10.2337/db22-0884.
12. Cantarelli E, Citro A, Marzorati S, Melzi R, Scavini M, Piemonti L. Murine animal models for preclinical islet transplantation: no model fits all (research purposes). *Islets.* 2013;5(2):79–86. https://doi.org/10.4161/isl.24698.
13. Hawthorne WJ, Salvaris EJ, Chew YV, et al. Xenotransplantation of genetically modified neonatal pig islets cures diabetes in baboons. *Front Immunol.* 2022;13:898948. https://doi.org/10.3389/fimmu.2022.898948.
14. Graham ML, Schuurman HJ. Validity of animal models of type 1 diabetes, and strategies to enhance their utility in translational research. *Eur J Pharmacol.* 2015;759:221–230. https://doi.org/10.1016/j.ejphar.2015.02.054.
15. Renner S, Braun-Reichhart C, Blutke A, et al. Permanent neonatal diabetes in INSC94Y transgenic pigs. *Diabetes.* 2013;62(5):1505–1511. https://doi.org/10.2337/db12-1065.
16. Liu M, Sun J, Cui J, et al. INS-gene mutations: from genetics and beta cell biology to clinical disease. *Mol Aspects Med.* 2015;42:3–18. https://doi.org/10.1016/j.mam.2014.12.001.
17. Kemter E, Denner J, Wolf E. Will genetic engineering carry xenotransplantation of pig islets to the clinic? *Curr Diab Rep.* 2018;18(11):103. https://doi.org/10.1007/s11892-018-1074-5.
18. Lindheimer F, Lindner MJ, Oos R, et al. Non-invasive in vivo imaging of porcine islet xenografts in a preclinical model with [⁶⁸Ga]Ga-exendin-4. *Front Nucl Med.* 2023;3:1157480. https://doi.org/10.3389/fnume.2023.1157480.
19. Kemter E, Cohrs CM, Schäfer M, et al. INS-eGFP transgenic pigs: a novel reporter system for studying maturation, growth and

vascularisation of neonatal islet-like cell clusters. *Diabetologia*. 2017; 60(6):1152–1156. https://doi.org/10.1007/s00125-017-4250-2.

20. Venturini M, Sallemi C, Marra P, et al. Allo- and auto-percutaneous intra-portal pancreatic islet transplantation (PIPIT) for diabetes cure and prevention: the role of imaging and interventional radiology. *Gland Surg*. 2018;7(2):117–131. https://doi.org/10.21037/gs.2017.11.12.

21. Blutke A, Renner S, Flenkenthaler F, et al. The Munich MIDY Pig Biobank − a unique resource for studying organ crosstalk in diabetes. *Mol Metab*. 2017;6(8):931–940. https://doi.org/10.1016/j.molmet.2017.06.004.

22. Arrojo e Drigo R, Ali Y, Diez J, Srinivasan DK, Berggren PO, Boehm BO. New insights into the architecture of the islet of Langerhans: a focused cross-species assessment. *Diabetologia*. 2015;58(10):2218–2228. https://doi.org/10.1007/s00125-015-3699-0.

23. Coe TM, Markmann JF, Rickert CG. Current status of porcine islet xenotransplantation. *Curr Opin Organ Transplant*. 2020;25(5):449–456. https://doi.org/10.1097/MOT.0000000000000794.

24. Shin JS, Kim JM, Min BH, et al. Pig-to-nonhuman primate (NHP) naked islet xenotransplantation. In: Miyagawa S, ed. *Xenotransplantation - New Insights*. IntechOpen; 2017. https://doi.org/10.5772/intechopen.69001.

25. Suszynski TM, Avgoustiniatos ES, Papas KK. Intraportal islet oxygenation. *J Diabetes Sci Technol*. 2014;8(3):575–580. https://doi.org/10.1177/1932296814525827.

26. Eriksson O, Eich T, Sundin A, et al. Positron emission tomography in clinical islet transplantation. *Am J Transplant*. 2009;9(12):2816–2824. https://doi.org/10.1111/j.1600-6143.2009.02844.x.

27. Eriksson O, Selvaraju R, Eich T, et al. Positron emission tomography to assess the outcome of intraportal islet transplantation. *Diabetes*. 2016; 65(9):2482–2489. https://doi.org/10.2337/db16-0222.

28. Brom M, Woliner-van der Weg W, Joosten L, et al. Non-invasive quantification of the beta cell mass by SPECT with ^{111}In-labelled exendin. *Diabetologia*. 2014;57(5):950–959. https://doi.org/10.1007/s00125-014-3166-3.

29. Renner S, Fehlings C, Herbach N, et al. Glucose intolerance and reduced proliferation of pancreatic beta-cells in transgenic pigs with impaired glucose-dependent insulinotropic polypeptide function. *Diabetes*. 2010;59(5):1228–1238. https://doi.org/10.2337/db09-0519.

30. Buerck LW, Schuster M, Oduncu FS, et al. LEA29Y expression in transgenic neonatal porcine islet-like cluster promotes long-lasting xenograft survival in humanized mice without immunosuppressive therapy. *Sci Rep*. 2017;7(1):3572. https://doi.org/10.1038/s41598-017-03913-4.